ORIGINAL PAPER

Nobuhito Imanaka · Tomohiro Ueda · Gin-ya Adachi

Tetravalent Zr^{4+} ion conduction in NASICON-type phosphate solids

Abstract The ionic conduction of mono-, di-, and tri-valent ions in solids is popular in solid state science and the next target ion species to migrate in solids are tetravalent ions. Here, a tetravalent cation conductor which shows high conductivity, comparable to the conductivity range of the representative divalent oxide anion conductors, was artificially designed by strictly selecting the constituent elements and the structure. The tetravalent ion conducting solid electrolyte proposed here shows considerable high ion conductivity and promising applications, such as in rechargeable batteries and chemical sensors for global environmental monitoring, are greatly expected.

Keywords Tetravalent · Ionic conduction · Solid electrolytes · Zirconium · Phosphates

Introduction

Ion conduction in solids is popular with monovalent species such as alkaline metal cations and divalent species such as alkaline earth cations [1, 2, 3, 4, 5] and oxide anions [6, 7, 8, 9, 10]. Recently, for multivalent ions higher than the divalent state, trivalent [11, 12, 13] and tetravalent cations [14] have been reported. However, the ion conductivity for cations higher than divalent state is appreciably below the practical application range. In this paper, a tetravalent cation conductor, whose ion conductivity is comparable to the conductivity region of divalent oxide anion conductors, was artificially designed by strictly selecting the structure and the constituent elements of the solid.

N. Imanaka (✉) · T. Ueda · G.-y. Adachi
Department of Applied Chemistry,
Faculty of Engineering, Osaka University,
2-1 Yamadaoka, Suita, Osaka 565-0871, Japan
E-mail: imanaka@chem.eng.osaka-u.ac.jp
Tel.: +81-6-68797353
Fax: +81-6-68797354

The target ion to conduct in solids is the tetravalent cation, and the ion migration in the structure is greatly influenced by the electrostatic interaction between the mobile tetravalent ion and the anions surrounding the tetravalent ion. For the purpose of reducing the interaction as much as possible to make tetravalent cations migrate in solids, the pathway for the tetravalent ion needs to have enough space for ion conduction and the space should be located three dimensionally. The NASICON (Na^+ ion Super Ionic CONductors) type and also the β-$Fe_2(SO_4)_3$ type structures (the latter slightly distorted from the NASICON structure), with a rhombohedral and a monoclinic symmetry, respectively, hold the three-dimensional network ion pathway which has been shown to be one of the suitable structures for multivalent ion conduction for divalent [1, 2, 3, 4, 5] and trivalent [13] cations.

The second issue to keep in mind is to properly choose the constituent elements. The higher the valency of the ion species in the structure, the stronger the electrostatic interaction appears between the cations and anions. For the purpose of realizing such surroundings so as to release the conducting cation to migrate smoother, a higher electrostatic interaction between the lattice forming cations and anions is necessary compared with the interaction between the mobile cations and the anions. Furthermore, since the mobile ion species is in a tetravalent state, the inclusion of lower valent cations than the tetravalent state must be excluded. The needs mentioned above mean that the solid should contain those elements whose valency state is pentavalent or higher. Also, the solid electrolytes should be stable enough in various atmospheres so as to prevent the reduction of the constituent elements which cause electronic conduction. From a stability point of view, candidate compounds are the oxide-based series whose stability has been already guaranteed.

In our previous letter [15], the tetravalent ion Zr^{4+} was selected as the target ion species to conduct and, as the lattice forming cations, the pentavalent ions of P^{5+} as well as Nb^{5+} were chosen to form a stable oxide solid,

and we reported an extraordinary high Zr^{4+} ion conduction in zirconium niobium phosphate [$ZrNb(PO_4)_3$]. In this paper, two NASICON-type solid electrolytes [$ZrM(PO_4)_3$, M = Nb or Ta] are prepared and the Zr^{4+} ion conducting characteristics in the solids are investigated in detail.

Experimental

Zirconium oxide (99.9%), diammonium hydrogenphosphate (99.99%), and niobium oxide (99.9%) or tantalum oxide (99.9%) were mixed in a stoichiometric ratio. The mixture was firstly heated at 1000 °C for 12 h and then at 1250 °C for 12 h in air. The resulting zirconium niobium or tantalum phosphates were made into pellets and the pellets were sintered at 1250 °C for 12 h in air.

X-ray powder diffraction analysis (Mac Science M18XHF diffractometer) was carried out using Cu-Kα radiation. Electrical conductivity was measured by both a.c. and d.c. methods with two platinum electrodes in the temperature range between 300 and 800 °C. The a.c. conductivity measurements were performed by an a.c. complex impedance method in the frequency region from 5 Hz to 13 MHz with a Hewlett Packard precision LCR meter (4192A). Before the a.c. conductivity measurements, pre-electrolysis treatment (700 °C, 3 V, 3 days in air) was conducted several times to remove the lower valent cation species [typically alkaline metal ion species such as Na^+ and K^+ were identified by electron probe microanalysis (EPMA)], which may appear in the starting materials as impurities and which may interfere with the conductivity characteristics. The termination of the electrolysis was assured by using the same conductivity value before and after the pre-electrolysis.

The polarization measurements were done by passing the d.c. current (1 μA) between the two platinum electrodes sandwiching the sample pellet and the voltage generated was monitored as a function of time in oxygen [$P(O_2)$: 10^5 Pa] and in nitrogen ($P(O_2)$: 50 Pa). The Pt dense electrode pellet was prepared by arc-melting platinum wire as a ball shape, which was then cut into a pellet shape. The oxygen pressure from $10^{-15.6}$ to 10^{-11} Pa and from 10^{-11} to 10^5 Pa were controlled by mixing CO-CO_2 and air (oxygen)-N_2 in an appropriate ratio, respectively. A wet air atmosphere from 0.6 to 20 vol% was prepared by applying water vapor saturated air between 0 and 60 °C. The d.c. electrolysis was performed for the pre-electrolyzed pellet at 700 °C and 3 V for 21 days in air. The cathodic surface of the pellets was examined by a scanning electron microscope (SEM, S-800, Hitachi) and by electron probe microanalysis (EPMA-1500, Shimadzu) after the electrolysis.

Results and discussion

The X-ray powder diffraction patterns for $ZrNb(PO_4)_3$ and $ZrTa(PO_4)_3$ are presented in Fig. 1 , together with the data for $NaZr_2(PO_4)_3$, which has a typical three-dimensional NASICON-type structure. The three peak profiles fit well and it was clear that both $ZrNb(PO_4)_3$ (hexagonal, lattice constants $a = 0.87$ nm, $c = 2.24$ nm) and $ZrTa(PO_4)_3$ (hexagonal, lattice constants $a = 0.87$ nm, $c = 2.23$ nm) possess exactly the NASICON-type structure (a very small amount of secondary peaks identified as $NbPO_5$ were also observed).

Identification of the macroscopic tetravalent Zr^{4+} ion migration was performed by the procedure described below. The electrical conductivity dependences on the oxygen pressure were measured for $ZrNb(PO_4)_3$, as shown in Fig. 2. The conductivity kept almost constant over a wide pressure region from 10^{-11} Pa to 10^5 Pa,
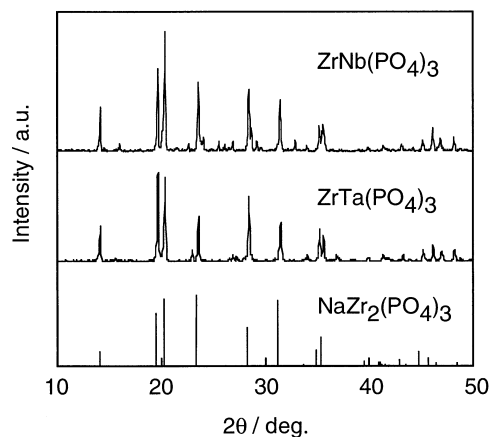

Fig. 1 X-ray powder diffraction patterns for $ZrNb(PO_4)_3$ and $ZrTa(PO_4)_3$ with that for $NaZr_2(PO_4)_3$, which has a typical three-dimensional NASICON-type structure
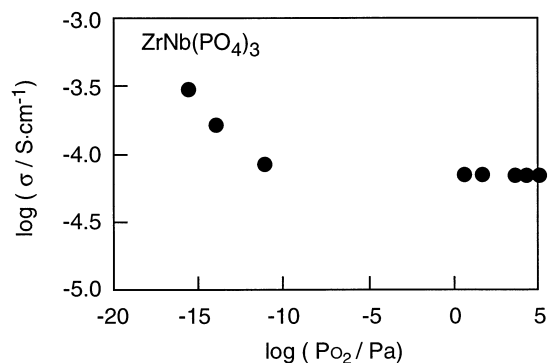

Fig. 2 The electrical conductivity dependences on the oxygen pressure for $ZrNb(PO_4)_3$ at 700 °C

indicating that the predominant migrating species is neither a hole nor an electron but an ion. At the oxygen pressure region below 10^{-11} Pa, the conductivity increases with the decrease of the pressure, showing the electronic conduction appearance in the $ZrNb(PO_4)_3$ solid electrolyte.

In addition, the time dependences of the d.c. to a.c. conductivity ratio (σ_{dc}/σ_{ac}) were monitored to investigate the polarizing behavior in both nitrogen [$P(O_2)$: 50 Pa] and oxygen [$P(O_2)$: 10^5 Pa] atmospheres; the results are presented in Fig. 3. Because an abrupt decrease in the ratio was similarly observed in both atmospheres, the oxide ion is excluded as the conducting candidate in the zirconium niobium phosphate solid, as described elsewhere [11, 12].

The d.c. polarization data in various wet atmospheres are listed in Table 1. For a water vapor content from 0 to 20 vol%, similar high polarization behavior was observed. In addition, similar polarization measurements were conducted by changing the operating temperature (Table 2) and a considerable high polarizing phenomenon was likewise obtained. The a.c. conductivity was also measured at 700 °C in the same water vapor region
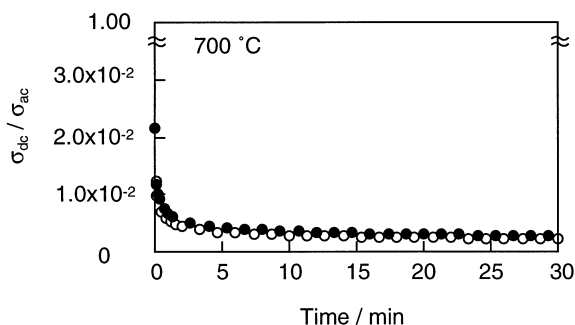
Fig. 3 The time dependences of the d.c. to a.c. conductivity (σ_{dc}/σ_{ac}) for ZrNb(PO$_4$)$_3$ in both nitrogen [$P(O_2)$: 50 Pa] (*filled circles*) and oxygen [$P(O_2)$: 10^5 Pa] (*open circles*) atmospheres (the values of the voltage applied are between 400 and 600 mV)

Table 1 The σ_{dc}/σ_{ac} ratio in a wet atmosphere at 700 °C

H$_2$O amount (vol%)	σ_{dc}/σ_{ac}
0.0	0.0030
0.6	0.0031
1.2	0.0035
2.3	0.0037
4.2	0.0040
7.3	0.0029
12.0	0.0042
20.0	0.0037

Table 2 The σ_{dc}/σ_{ac} ratio in a 20 vol% H$_2$O atmosphere at various temperatures

Temperature (°C)	σ_{dc}/σ_{ac}
500	0.0053
600	0.0031
700	0.0037
800	0.0047

Fig. 4 The a.c. conductivity of ZrNb(PO$_4$)$_3$ measured at 700 °C with a water vapor content between 0 and 20 vol%
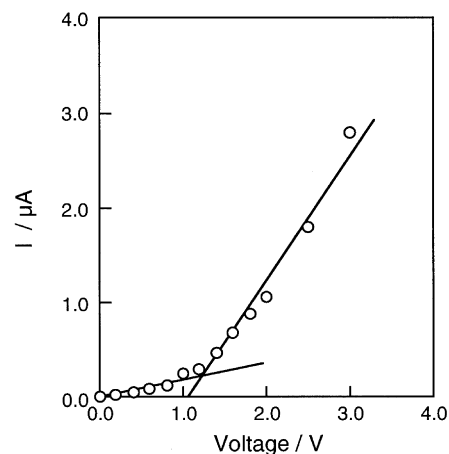
Fig. 5 The I vs. V characteristics for ZrNb(PO$_4$)$_3$

Table 3 The results of EPMA spot analyses before and after the electrolysis [two areas (1 and 2) were investigated on the cathodic surface]

Element	Atom %			
	Before	After		
		Cathode (area 1)	Cathode (area 2)	Anode
Zr	20.8	60.9	50.7	20.2
Nb	15.9	3.2	2.6	16.9
P	63.2	35.9	45.8	62.9

and the results are presented in Fig. 4. The water vapor variation does not interfere with the a.c. conductivity. From these results the mobile ion candidates in the zirconium niobium phosphate are limited only to the cation species Zr^{4+}, Nb^{5+}, or P^{5+}. The ion transference number estimated from the polarization measurements in Fig. 3 is higher than 0.999 and ZrNb(PO$_4$)$_3$ was found to be a pure ion conductor.

In order to directly and exactly identify the conducting cation species, a d.c. electrolysis (700 °C, 3 V, 21 days in air) was carried out by sandwiching the ZrNb(PO$_4$)$_3$ pellet between two platinum electrodes in a similar manner to that reported in our previous papers [11, 12, 13] [the decomposition voltage of ZrNb(PO$_4$)$_3$ was clarified to be ca. 1.2 V from the electrolysis experiment presented in Fig. 5]. Here, the higher voltage in comparison to the decomposition voltage was applied in order to continuously supply the mobile cations at the anode and also so that the macroscopic cation conduction can proceed. After the electrolysis, deposits were clearly observed on the cathodic surface of ZrNb(PO$_4$)$_3$ by mapping with EPMA. From the spot analyses (two
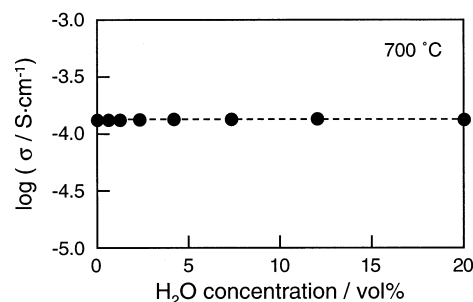
areas) of the deposits appearing on the cathode (Table 3), only the Zr ratio increases more than twice, while the ratios for Nb and P reduce considerably. In contrast, the ratios for Zr, Nb, and P at the anode are almost similar to the ZrNb(PO$_4$)$_3$ bulk before the electrolysis. The results described above clearly mean that a predominant element in the deposits is not Nb nor P but Zr. Furthermore, from the cross-sectional line analysis of the electrolyzed pellet (Fig. 6), a high amount of Zr segregation was clearly observed near the cathodic surface and highlighted as a shaded area, while any Nb or P increase in the content was not observed, demonstrating that the predominant conducting cation species is only
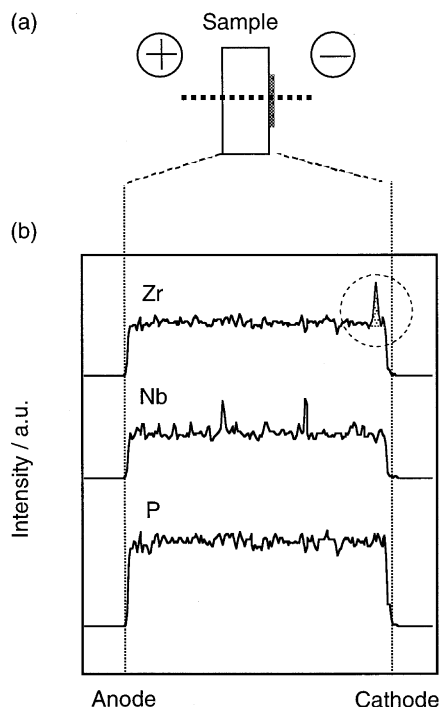
Fig. 6 a The electrolysis set-up and **b** the EPMA line analysis results for the elements Zr, Nb, and P. The Zr segregation is shown as the *highlighted area* in the *broken circle*. The analysis was conducted in the direction from anode to cathode along the broken line in **a**

Fig. 7 The temperature dependences of the tetravalent Zr^{4+} ion conductivity of $ZrNb(PO_4)_3$ (*solid circles*) and $ZrTa(PO_4)_3$ (*open squares*) with the data for representative Na^+ ion conducting NASICON (*two dots-dash curve*) and β-Al_2O_3 (*full curve*), $Mg_{0.7}(Zr_{0.85}Nb_{0.15})_4P_6O_{24}$ (*dashed curve*) [16], $Sc_2(WO_4)_3$ (*single dot-dash curve*) [12], and the tetravalent ion ($Zr_2O(PO_4)_2$) conductor (*dotted curve*) [14]

tetravalent Zr^{4+}. The above-mentioned phenomena clearly indicate the fact that tetravalent Zr^{4+} ions, generated by the decomposition, continuously migrate in the $ZrNb(PO_4)_3$ bulk by electrolysis from the anode to cathode direction and deposit on the cathodic surface.

The temperature dependences of the tetravalent Zr^{4+} ion conductivities of the $ZrNb(PO_4)_3$ and $ZrTa(PO_4)_3$ solids are presented in Fig. 7, together with representative data for the Na^+ ion conducting NASICON and β-Al_2O_3, $Mg_{0.7}(Zr_{0.85}Nb_{0.15})_4P_6O_{24}$ [16], $Sc_2(WO_4)_3$ [12], and the tetravalent ion conductor $Zr_2O(PO_4)_2$ reported previously [14]. Between the two $ZrNb(PO_4)_3$ and $ZrTa(PO_4)_3$ solids, $ZrNb(PO_4)_3$ shows approximately three times as high a conductivity as that for $ZrTa(PO_4)_3$, indicating that the $ZrNb(PO_4)_3$ solid electrolyte is more suitable compared with the $ZrTa(PO_4)_3$ solid. The first demonstration of a pure tetravalent cation conductor was reported for $Zr_2O(PO_4)_2$ [14]. However, the Zr^{4+} ion conductivity is lower than 10^{-5} S cm^{-1} up to the operating temperature of 800 °C. The Zr^{4+} ion conductivity of the present $ZrNb(PO_4)_3$ solid is more than two orders of magnitude higher at 400 °C and 30 times as high as that of $Zr_2O(PO_4)_2$ at 800 °C. In addition, the tetravalent Zr site replacement for Nb^{5+} in zirconium niobium phosphate was effective enough to decrease the activation energy for the Zr^{4+} ion migration from 78.9 to 56.2 kJ mol^{-1}. The ionic conductivity of $ZrNb(PO_4)_3$ exceeds that of $Sc_2(WO_4)_3$, which shows the highest trivalent ion conductivity among the
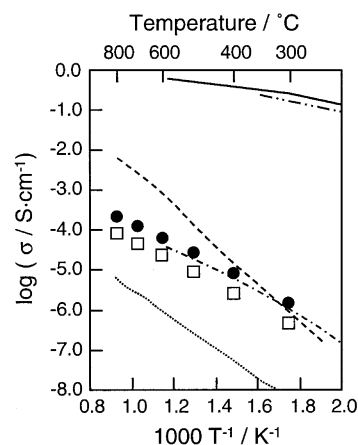
$Sc_2(WO_4)_3$ type series. In addition, the Zr^{4+} ion conductivity in $ZrNb(PO_4)_3$ is also comparable to divalent oxide anion conductors of stabilized zirconias like yttria-stabilized zirconia (YSZ) [9] and calcia-stabilized zirconia (CSZ) [9].

Conclusions

The tetravalent Zr^{4+} ion conducting solid electrolyte, which shows a comparable ion conductivity to the trivalent ion conductor $Sc_2(WO_4)_3$ and also to the O^{2-} ion conductor series, was successfully obtained for the $ZrNb(PO_4)_3$ polycrystal. The considerable higher Zr^{4+} ion conduction was realized by strictly selecting the structure which possesses a three-dimensional ion pathway such as the NASICON type and also choosing the constituent elements which have the valency state higher than the migrating ion valency in the tetravalent state.

References

1. Ikeda S, Takahashi M, Ishikawa J, Ito K (1987) Solid State Ionics 23:125
2. Nomura K, Ikeda S, Ito K, Einaga H (1992) Bull Chem Soc Jpn 65:3221

3. Nomura K, Ikeda S, Ito K, Einaga H (1993) Solid State Ionics 61:293
4. Imanaka N, Okazaki Y, Adachi G (1999) Chem Lett 939
5. Imanaka N, Okazaki Y, Adachi G (2000) J Mater Chem 10:1431
6. Takahashi T, Iwahara H (1978) Mater Res Bull 13:1447
7. Subbarao EC, Sutter PH, Hrizo J (1965) J Am Ceram Soc 48:443
8. Kudo T, Obayashi H (1976) J Electrochem Soc 123:415
9. Strickler DW, Carlson WG (1964) J Am Ceram Soc 47:122
10. Lacorre P, Goutenoire F, Bohnke O, Retoux R, Laligant Y (2000) Nature 404:856
11. Kobayashi Y, Egawa T, Tamura S, Imanaka N, Adachi G (1997) Chem Mater 9:1649
12. Imanaka N, Kobayashi Y, Fujiwara K, Asano T, Okazaki Y, Adachi G (1998) Chem Mater 10:2006
13. Tamura S, Imanaka N, Adachi G (1999) Adv Mater 11:1521
14. Imanaka N, Ueda T, Okazaki Y, Tamura S, Hiraiwa M, Adachi G (2000) Chem Lett 452
15. Imanaka N, Ueda T, Adachi G (2001) Chem Lett 446
16. Imanaka N, Okazaki, Y, Adachi G (2000) Electrochem Solid-State Lett 3:327